Magnetization dynamics: A study of the ferromagnet/antiferromagnet interface and exchange biasing

R. E. Camley,[a] B. V. McGrath, and R. J. Astalos
Department of Physics, University of Colorado at Colorado Springs, Colorado Springs, Colorado 80933-7150

R. L. Stamps, Joo-Von Kim, and Leonard Wee
Department of Physics, University of Western Australia, Nedlands, WA 6907, Australia

(Received 9 October 1998; accepted 9 November 1998)

We use a method which employs a dynamic calculation of magnetization motion to find both the static configuration and the spin wave excitations in a ferromagnet/antiferromagnet layered structure. Our results for the static structure are similar to those found in Koon's model; i.e., in zero applied field the ferromagnet points perpendicularly to the easy axis of the antiferromagnet, and the surface spins of the antiferromagnet are in a surface spin flop configuration. The calculated hysteresis curve for this structure shows a small exchange bias, in agreement with typical experimental results. We explore how this bias depends on the parameters of the antiferromagnet and on the nature of the interface coupling. We further examine models for antiferromagnets with both compensated and uncompensated surfaces. We show that the structure calculated by Koon is unstable at higher reversed magnetic fields but that this instability can be suppressed by an easy-plane anisotropy. © *1999 American Vacuum Society.* [S0734-2101(99)00404-2]

I. INTRODUCTION

When a ferromagnetic film is in contact with an antiferromagnet a number of changes can occur to the hysteresis curve associated with the ferromagnet:

(1) The hysteresis curve may be shifted so that it appears that the antiferromagnet produces an effective field acting on the ferromagnet. This field is typically a few hundred Gauss or less.
(2) The width of the hysteresis curve can be substantially increased. The increase can extend to a few kG.

There are a number of additional features. The shift disappears if the antiferromagnet film is too thin, 20–30 monolayers typically. Also, the size of the effect decreases with increasing temperature and vanishes near the Neel temperature for the antiferromagnet. The effects above are known generally by the terminology of exchange biasing or exchange anisotropy.

The precise mechanism for exchange biasing has remained unclear for over 40 years.[1–4] One problem, in particular, concerns the size of the effect. The effective exchange fields coupling the ferromagnet to the antiferromagnet are expected to be on the order of 100–1000 kG. Yet the size of the effective field seen in the hysteresis curve is several orders of magnitude smaller.

Recently, there have been several proposals to explain the size of the effect. In particular, Koon discussed a model where a ferromagnet coupled to an antiferromagnet with a compensated surface could produce a small shift in the hysteresis curve.[5] In contrast, other models depend on a small asymmetry between the number of up and down spins at the surface of the antiferromagnet.[6]

[a]Electronic mail: rcamley@brain.uccs.edu

In this article we explore the exchange biasing issue for antiferromagnets with both compensated and uncompensated surfaces. We use a theoretical method—integration of the dynamic equations of motion—which is fundamentally different from that of energy minimization, and find that the spin configuration in Koon's model becomes unstable at a critical value of the external magnetic field.[7,8] We explore a recent suggestion[9] that the instability is a possible mechanism for the enhanced hysteresis seen in ferromagnet/antiferromagnet structures. In addition we also explore how the shift and width of the hysteresis curve depend on the angle between the applied field and the easy axis of the antiferromagnet, a topic which has been investigated experimentally recently.[10,11]

II. THEORETICAL APPROACH

We use a numerical scheme which calculates the dynamic motion of the spins to find the equilibrium spin configuration. One begins by writing the energy density for the coupled structure. This energy density defines the effective field acting on each layer of the ferromagnet and on the two sublattices of the antiferromagnet. The effective field is then used to find the coupled equations of motion for the spins in each layer. The system is then given some initial configuration and allowed to evolve in time according to the equations of motion. As a result of some damping, the system evolves to a structure where the spins in each layer are pointing along their local effective field direction. This effectively finds a minimum energy state.

We model the system as a set of interacting layers. The total energy density of the ferromagnet involves the exchange energy, anisotropy energy, and Zeeman and dipolar energies:

$$E_f = -\sum_{i=1}^{N_f-1}\left(\frac{A_f}{d^2}\right)\mathbf{a}^{(i)}\cdot\mathbf{a}^{(i+1)} - \sum_{i=1}^{N_f} K_i (a_z^{(i)})^2 - \sum_{i=1}^{N_f}(\mathbf{H}+\mathbf{h}^{(i)})\cdot\mathbf{a}^{(i)}\mathbf{M}^{(i)}. \quad (1)$$

Here $\mathbf{M}^{(i)}$ is the magnetization vector in layer i, K_i the uniaxial in-plane anisotropy constant for layer i, and A_f is the exchange coupling constant between layers in the ferromagnet. The quantity $\mathbf{h}^{(i)}$ is a small fluctuating magnetic field arising from the dipole field of the precessing spins. The distance between magnetic layers is d. For convenience, we have changed to unitless variables for the magnetization, i.e., $\mathbf{a}^{(i)} = \mathbf{M}^{(i)}/M^{(i)}$. N_f is the number of ferromagnetic layers.

In addition there is the interfacial exchange energy density between the ferromagnet and antiferromagnet:

$$E_{\text{inter}} = -\left(\frac{A_{\text{inter}}}{d^2}\right)\mathbf{a}^{(N_f)}\cdot(\mathbf{b}^{(N_f+1)} + \mathbf{c}^{(N_f+1)}). \quad (2)$$

The normalized magnetizations for the two sublattices of the antiferromagnet in layer i are represented by $\mathbf{b}^{(i)}$ and $\mathbf{c}^{(i)}$. Finally there is the energy density terms associated with the antiferromagnet.

$$E_{af} = -\sum_{i=N_f+1}^{N_f+N_{af}-1}\left(\frac{A_{af}}{d^2}\right)(\mathbf{b}^{(i)}\cdot\mathbf{c}^{(i+1)} + \mathbf{c}^{(i)}\cdot\mathbf{b}^{(i+1)} + 2\mathbf{b}^{(i)}\cdot\mathbf{c}^{(i)}) - \sum_{i=N_f+1}^{N_f+N_{af}} K_i[(b_z^{(i)})^2 + (c_z^{(i)})^2] - \sum_{i=N_f+1}^{N_f+N_{af}}(\mathbf{H}+\mathbf{h}^{(i)})\cdot(\mathbf{b}^{(i)}M^{(i)} + \mathbf{c}^{(i)}M^{(i)}). \quad (3)$$

The energy density is used to derive $\mathbf{H}_{\text{eff}}$, the effective field acting on layer (i). This is through the definition $\mathbf{H}_{\text{eff}} = -\partial E_{\text{total}}/\partial \mathbf{M}^{(i)}$. The total effective field is thus a sum of exchange, anisotropy, dipolar, and external fields. We assume that the main contribution to the dipole field $\mathbf{h}^{(i)}$ is the demagnetizing field of a thin layer acting on itself. Thus $\mathbf{h}^{(i)} = 4\pi M^{(i)} a^{(i)}{}_y$ in the ferromagnetic layers for example. This approximation works well for thin films in the long wavelength limit when $qD \ll 1$ where D is the thickness of the film and q is component of the spinwave wave vector parallel to the surface.[12]

The equations of motion for a layer in the ferromagnet are now given by

$$\frac{d\mathbf{a}^{(i)}}{dt} = \gamma \mathbf{a}^{(i)} \times \mathbf{H}_{\text{eff}} + \left(\frac{\alpha}{M^{(i)}}\right)\mathbf{a}^{(i)} \times \mathbf{a}^{(i)} \times \mathbf{H}_{\text{eff}}. \quad (4)$$

Similar equations hold for the b and c sublattices in the antiferromagnet. In Eq. (4) the first term on the right represents the torque produced on a spin in layer i by an effective magnetic field. The second term is the Landau–Lifshitz damping term which allows the spin to decay to the local field direction, but keeps the magnitude of the spin constant. Here γ is the gyromagnetic ratio and α is the effective damping parameter.

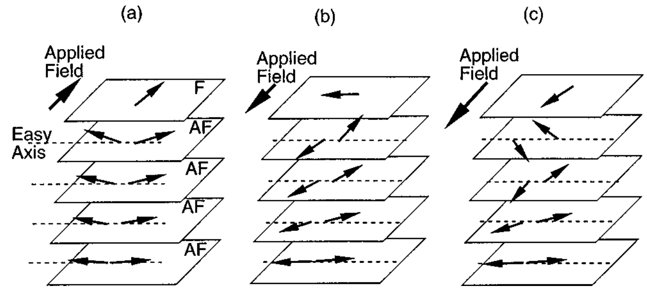

FIG. 1. Schematic illustration of the spin configurations in the ferromagnet/antiferromagnet interface. The angle θ gives the angle between the easy axis of the antiferromagnet and the applied field.

The coupled set of equations is then given an initial state and iterated forward in time through a Runge–Kutta method. The equilibrium position is found by using a large value for the damping constant α. This forces the system to dynamically relax to the ground state. Unless otherwise indicated, the standard parameters for our calculation are as follows: $N_f = 20$, $N_{af} = 30$, $A_f = 2\times10^{-6}$ erg/cm^2, $A_{af} = -2\times10^{-7}$ erg/cm^2, $A_{\text{inter}} = 2\times10^{-6}$ erg/cm^2, $K_f = 10^3$ erg/cm^3, $K_{af} = 3\times10^6$ erg/cm^3, $M_f = 1.7$ kG, $M_{af} = 0.6$ kG.

We note that our calculation is fundamentally different from the method used by Koon. Koon's results were based on a model that involved energy minimization in a plane, i.e., the magnetic moments in each layer of the ferromagnet and antiferromagnet were restricted to lie in planes parallel to the surface of the structure. Since we are dealing with a system where spin motions are allowed in any of the three dimensions, our model allows for a more general configuration and as a result obtains different results in some cases.

III. RESULTS

We first describe the spin configurations involved in the hysteresis curves. In Koon's model and in our results the ferromagnet spins are perpendicular to the easy axis of the antiferromagnet in the absence of an external field H. As a result of the coupling to the ferromagnet, the antiferromagnet has a structure that is similar to a surface spin flop configuration. Recent neutron results,[13] in fact, show a spin configuration consistent with the calculations. The general structure for a large positive field H is illustrated in Fig. 1(a). As the field is reversed, the magnetic moments in the ferromagnet rotate and build up a twisted state in the antiferromagnet as shown in Figs. 1(b) and 1(c).

We now investigate the stability of the twisted state in the antiferromagnet. In Fig. 2 we show the hysteresis curves calculated by the energy minimization method and by the dynamic calculation. All curves are calculated for the same parameters, except that an easy-plane anisotropy has been added to some of the dynamic calculations. All the methods agree in the general shape of the curve. The energy minimization method shows a shift in the magnetization curve as a twist is built into the antiferromagnet, i.e., the $M=0$ state occurs at about 2 kG rather than at zero applied field. In the energy minimization method the twisted state becomes un-

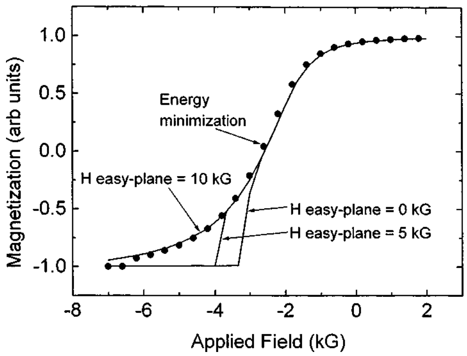

FIG. 2. Hysteresis curves calculated by the energy minimization method and the dynamic method. The dynamic method calculations are done for different values of easy-plane anisotropy showing how the instability may be suppressed by increasing the easy-plane anisotropy. The dotted curve represents the two-dimensional energy minimization results. (Only half the hysteresis curves are shown.) We use standard parameters except that $A_{\mathrm{inter}} = 3\times10^{-7}$ erg/cm^2. The angle $\theta = 70°$.

stable just past 6 kG. In contrast the dynamic calculations shows that the structure becomes unstable at different critical fields which depend on the easy-plane anisotropy. In the dynamic calculations the instability is associated with large out of plane motions for the individual magnetic moments. If we prevent these motions, we should expect that the instability could be eliminated. As is seen in the figure, the precise critical field depends on the value of the easy-plane anisotropy, and for sufficiently high values, the instability can be suppressed.

It is characteristic of our results that the shape, shift, and width of the hysteresis curve depends on the angle between the easy axis and the applied field. In a set of recent experiments Ambrose *et al.* have carefully measured hysteresis curves as a function of angle.[10,11] They obtained results on how the width and shift of the hysteresis curve depend on the angle of orientation for the applied magnetic field. Furthermore it has recently been suggested that the enhanced width in ferromagnet/antiferromagnet structures comes precisely from the initial building of the twist and then its subsequent instability.[9] It is therefore of interest to see how our theoretical results compare with the experiments.

In Fig. 3 we examine how the width of the hysteresis curve depends on angle. We use our standard parameters for this calculation except that the interface coupling is $A_{\mathrm{inter}} = |A_{af}|/2$. We see that the width is largest for $\theta = 90°$ and smallest for $\theta = 0°$ or 180°. As the angle is changed from 90° the shape of the curve changes from rectangular to a more rounded diagonal shape. The theoretical results agree qualitatively with the experimental ones if we assume that the experimental process of training the system by application of a large field at high temperature essentially encourages the formation of domains in the antiferromagnet with the easy axis perpendicular to the applied field.

The curves in Fig. 3 are symmetric about $H = 0$, i.e., there is no shift in the hysteresis curve. This is to be expected because the magnetic structure becomes unstable for large negative fields and as a result the hysteresis curve is not

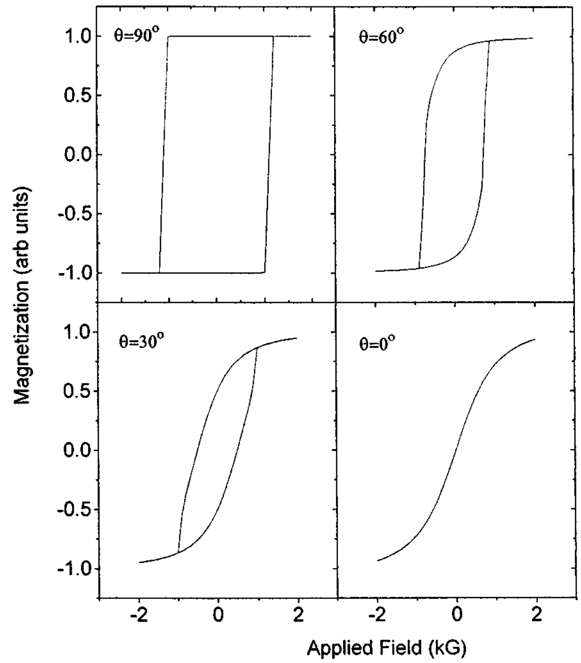

FIG. 3. Hysteresis curves for different angles θ between the easy axis and the applied field. The easy-plane anisotropy is zero so the width of the curve depends on the instability of the twisted state in the antiferromagnet. We use standard parameters except $A_{\mathrm{inter}} = |A_{af}|/2$.

reversible. As pointed out above, the instability can be suppressed if there is sufficient easy-plane anisotropy in the antiferromagnet. In fact, a number of other parameters encourage stability as well—an increased number of layers in the antiferromagnet and a stronger value for interface coupling. The calculation for Fig. 4 therefore uses $N_{af} = 50$, $A_{\mathrm{inter}} = 4\times10^{-7}$ erg/cm^2, and $H_{\mathrm{easy\ plane}} = 15$ kG. In Fig. 4 we plot magnetization curves for different angles between the external field and the easy axis. The shift is largest when the angle θ is close to 90°, goes to zero for $\theta = 0°$, and then is negative for negative angles. Again this is consistent with the experimental results.

While we have matched the general trends found experimentally, we did it by exploring the two features—width and

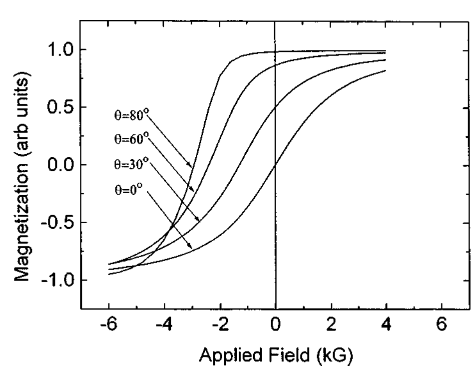

FIG. 4. Hysteresis curves for different angles θ between the easy axis and the applied field. The easy-plane anisotropy is large (15 kG) so the instability is suppressed. All the curves are now reversible and shifted. The calculation is done with standard parameters except that $N_{af} = 50$, $A_{\mathrm{inter}} = 4\times10^{-7}$ erg/cm^2, and $H_{\mathrm{easy\ plane}} = 15$ kG.

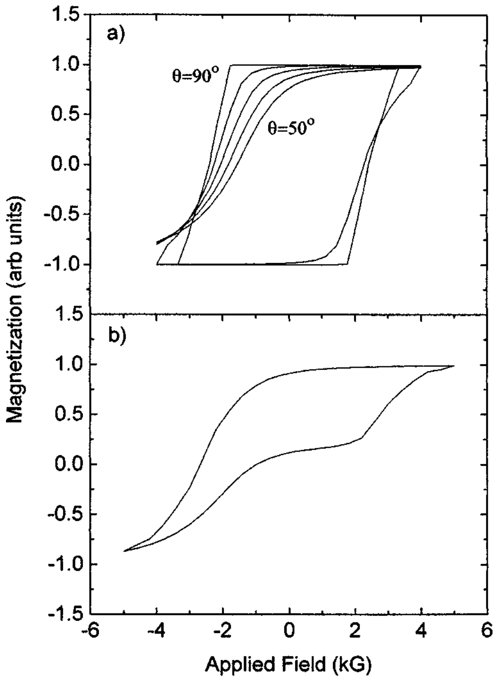

FIG. 5. Hysteresis results for an intermediate case where both reversible and nonreversible magnetization curves are found depending on the angle θ. (a) shows the hysteresis curves for angles which vary, in 10° increments, from 90° to 0°. (b) shows the average of the hysteresis curves from part (a). The special parameters for this calculation are $H_{\text{easy plane}}=15\,\text{kG}$ and $A_{\text{inter}}=3\times10^{-7}\,\text{erg/cm}^2$.

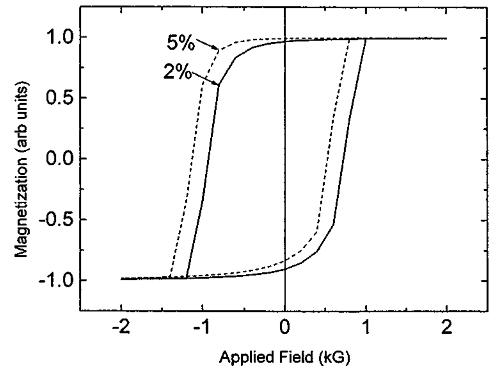

FIG. 6. Hysteresis curves for slightly uncompensated antiferromagnetic surfaces. The numbers indicate the percentage enhancement of the number of up spins over down spins at the surface of the antiferromagnet. The special parameters for this calculation are $H_{\text{easy plane}}=0$ and $A_{\text{inter}}=1\times10^{-7}\,\text{erg/cm}^2$, also $0=70°$.

shift of the hysteresis curve—separately. That is, we obtained in the theoretical results either an increase in the width of the hysteresis curve or a shift in the center of the hysteresis curve. We now want to examine whether both a shift and an increase in the coercive field are possible simultaneously within the theoretical calculations. One possibility is that the experimental situation has many different domains with the easy axes in each domain having a different orientation with respect to the applied field. We can model this situation by averaging the hysteresis curves over angles θ. In Fig. 5(a) we plot the hysteresis curves for different angles. We have chosen parameters ($H_{\text{easy plane}}=15\,\text{kG}$ and $A_{\text{inter}}=3\times10^{-7}\,\text{erg/cm}^2$) so that the curve is reversible for some angles and is not reversible for other angles. When we average the hysteresis curves, we see in Fig. 5(b) a shifted and wider hysteresis curve. The curve however, has a distinctly asymmetric shape. We note that curves close to this shape have been seen if ferromagnet/antiferromagnet structures recently.

As a final example we consider what might happen if there is a slight imbalance in the number of up and down spins at the surface of the antiferromagnet. In Fig. 6 we present results for the case where the number of up spins in the antiferromagnet (those aligned with $+x$ axis) is 2% or 5% larger than the number of down spins. We first note that for this structure the natural direction for the ferromagnet is not perpendicular to the easy axis as was the case in Fig. 1. The magnetization in the ferromagnet is now tilted somewhat toward the $+x$ axis. For our parameters, ($H_{\text{easy plane}}=0$ and $A_{\text{inter}}=1\times10^{-7}$) the natural angle (i.e., the angle at $H=0$) is 70°. The hysteresis curve in Fig. 6 shows both an enhanced width—due to the instability of the twisted state in the antiferromagnet—and a shift due to the asymmetry in the number of surface spins. The shift, on the order of a few hundred Gauss, is consistent with typical experimental results.

IV. SUMMARY AND CONCLUSIONS

We have explored the behavior of the hysteresis curves for a structure composed of a coupled ferromagnet and antiferromagnet. In contrast to Koon's work, our method is based on a time-dependent calculation and not on an energy minimization method. Our results show that Koon's model where the exchange bias is caused by a twist in the antiferromagnet is incomplete in that Koon's spin configuration can become unstable at certain applied fields. We explore different possibilities for stabilizing the twisted state and find that strong interfacial coupling combined with some easy-plane anisotropy can suppress the transition from the twisted state. Our results for the behavior of the width of the hysteresis curves as a function of angle qualitatively agree with recent experiments.

The dynamic method developed here can be used to calculate spin wave frequencies in both the ferromagnet and antiferromagnet as well as the static hysteresis curves. The results of these calculations will be presented elsewhere.[7]

ACKNOWLEDGMENT

The work at Colorado Springs was supported by US ARO under Grant No. DAAG55-98-0294.

[1]W. H. Meiklejohn and C. P. Bean, Phys. Rev. **105**, 904 (1957).
[2]J. Nogues, D. Lederman, T. J. Moran, and I. K. Schuller, Phys. Rev. Lett. **76**, 4624 (1996).
[3]A. P. Malozemoff, Phys. Rev. B **35**, 3679 (1987).
[4]D. Mauri, H. C. Siegmann, P. S. Bagus, and E. Kay, J. Appl. Phys. **62**, 3047 (1987).
[5]N. C. Koon, Phys. Rev. Lett. **78**, 4865 (1997).
[6]K. Takanao, R. H. Kodama, and A. E. Berkowitz, 7th Joint MMM-

Intermag Conference, Abstract EA-03 (1998).
[7]R. E. Camley and R. J. Astalos, J. Magn. Magn. Mater. (in press).
[8]T. C. Schulthess and W. H. Butler, Phys. Rev. Lett. **81**, 4516 (1998).
[9]M. D. Stiles and R. D. McMichael, Phys. Rev. B (in press).
[10]T. Ambrose, R. L. Sommer, and C. L. Chien, Phys. Rev. B **56**, 83 (1997).
[11]X. W. Wu, T. Ambrose, and C. L. Chien, Appl. Phys. Lett. **72**, 2176 (1998).
[12]R. L. Stamps, Phys. Rev. B **49**, 339 (1994).
[13]Y. Ijiri, J. A. Borchers, R. W. Erwin, and S.-H. Lee, 7th Joint MMM-Intermag Conference, Abstract EA-02 (1998).